ELSEVIER

Catalysis Today 54 (1999) 559–567

CATALYSIS TODAY

www.elsevier.com/locate/cattod

Uncatalyzed and catalyzed NO and N_2O reaction using various catalysts and binary barium mixtures supported on activated carbon

Sónia A. Carabineiro [a,*], F. Brás Fernandes [b], Joaquim S. Vital [a],
Ana M. Ramos [a], Isabel F. Silva [a]

[a] *Departamento de Química, C.Q.F.B., Universidade Nova de Lisboa, Faculdade de Ciências e Tecnologia, 2825–114 Caparica, Portugal*
[b] *Departamento de Ciência dos Materiais, CENIMAT, Universidade Nova de Lisboa, Faculdade de Ciências e Tecnologia, 2825–114 Caparica, Portugal*

Abstract

The kinetics of the reaction of NO and N_2O with activated carbon, without catalyst, and impregnated with precursor salts of Mg, Mn, Ba, Pb, Cu, Ni, Fe and Co and their binary mixtures was investigated. The conversion of NO and N_2O was studied (300°C–900°C) using a TGA apparatus and a fixed-bed reactor. The reactor effluents were analyzed using a GC/MS on line. The best synergetic effects were observed for samples doped with Ba + Pb, Ba + Fe, Ba + Cu, Ba + Mn, and Cu + Mn. Adsorption of NO and N_2O (20°C–100°C) increased considerably in the presence of catalysts, but binary mixtures had no synergistic effects. In situ XRD was an useful tool for interpreting catalyst behavior and identifying phases during reaction conditions. ©1999 Elsevier Science B.V. All rights reserved.

Keywords: NO reduction; Catalysis; Kinetics; X-ray diffraction; Adsorption

---

1. Introduction

NO removal from exhaust streams of various combustion sources has become increasingly important in the past few years [1–14]. Recently, catalytic reduction of NO, with carbons as reducing reagents, has been intensively investigated [2–8,10–12,14].

The reaction depends significantly on the composition of the catalyst and the nature of the reacting carbon [8]. The major factors that influence the rates of reaction with carbon are

1. The concentration of active sites on the carbon surface;
2. The crystallinity and the structure of the carbon; and
3. The diffusion of reactive gases to the active sites.

In an attempt to understand and propose a mechanism for catalytic carbon gassification with oxygen, carbon dioxide, water vapor and hydrogen, McKee studied the effects of alkaline, alkaline earth and transition metals using TGA/DTA and hot-stage microscopy [15,16]. The author concluded that the catalytic process involves an oxidation–reduction cycle. The oxidation state of the metal determines its performance, and the ability of the precursor to be reduced by carbon to a lower oxidation state, is an important factor [15,16]. Also, the ability of the catalyst to melt and spread on carbon surface promotes catalyst/carbon contact and reactivity is enhanced [1,15–19].

Illán-Gomez et al. reported that alkaline, alkaline earth and transition metal catalysts seem to enhance NO chemisorption to different extents and they play an important role in redox cycle, which transfers oxygen from the catalyst surface to the carbon surface to

---

[*] Corresponding author.

PII: S0920-5861(99)00218-7

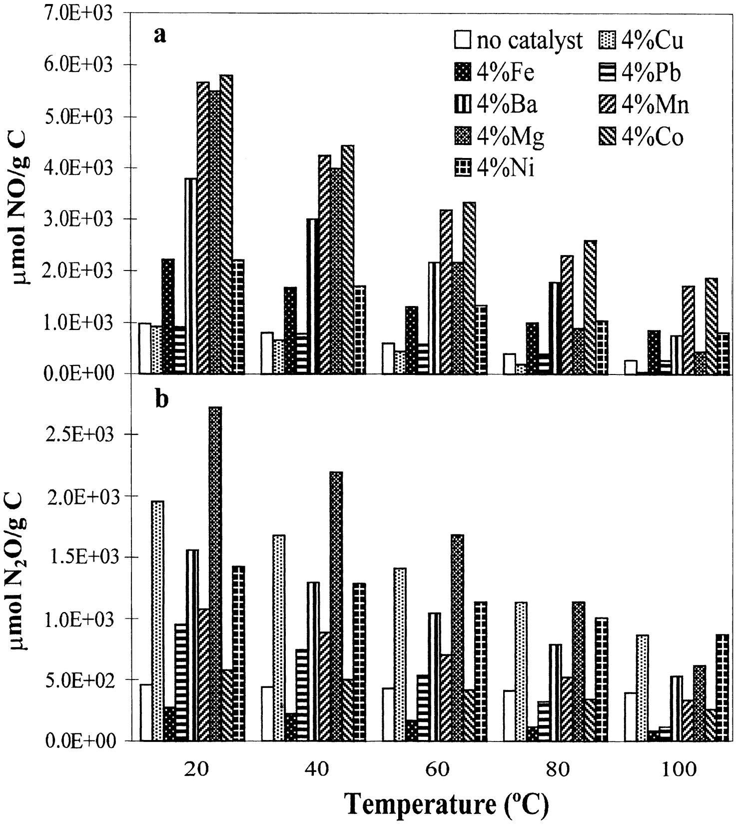

Fig. 1. NO (a) and N_2O (b) adsorption for carbon parent sample and samples doped with several catalysts, at different temperatures.

produce CO_2 and CO [4–8]. This mechanism is analogous to the one occurring in other carbon gassification reactions [15,16].

According to earlier studies of Aarna and Suuberg, at low temperatures, dissociative NO chemisorption results in the formation of a carbon–oxygen complex and the decomposition of these complexes (at higher temperatures) leads to production of CO_2 and CO [13]. In recent studies, Illán-Gomez et al. reported that the analysis of the reaction products reveals a mechanism for catalytic NO reduction with three stages [4–8]:

1. At low temperatures, N_2 and/or N_2O are the only products. Oxygen is retained on the catalyst/carbon surface.
2. Above 300°C, N_2 continues to evolve, but CO_2 evolution occurs and the rate of NO reduction increases.
3. Above 500°C, N_2 evolution becomes constant and CO becomes dominant.

The active sites that retain and transfer oxygen to carbon are different, depending on the nature of the chemical species involved in each case [5–8]. In a recent work, Rodriguez-Mirasol et al. [3,9] reported the results obtained for N_2O decomposition. Authors observed that N_2O is more readily reduced on carbon surface than NO. The gas products observed were N_2 and CO_2, according to this model

$$N_2O + C \rightarrow N_2 + C(O)$$

$$N_2O + C(O) \rightarrow N_2 + CO_2$$

N_2O seems to promote more less-stable oxygen surface complexes that decompose yielding CO_2 and vacant sites. The presence of catalysts seems to favor the production of the oxygen surface complexes, which can easily be scavenged by CO to produce CO_2 and vacant sites, thus enhancing N_2O decomposition [3,9].

The aim of the present work is to study the behavior of several metals as catalysts and their binary mixtures

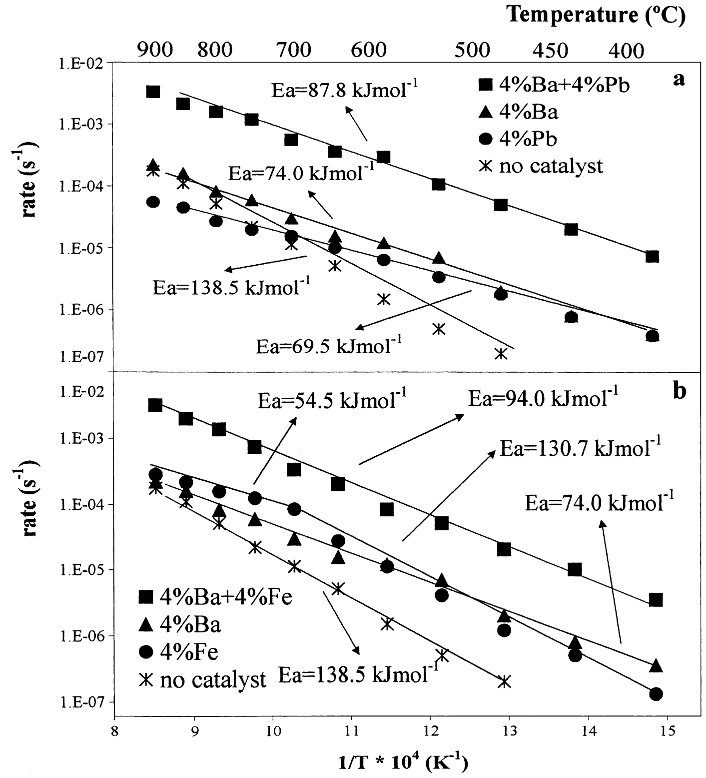

Fig. 2. Arrhenius plots for carbon gassification in NO for carbon parent sample and samples doped with Ba, Pb, and Ba + Pb mixture (a), and samples doped with Ba, Fe, and Ba + Fe mixture (b).

for C/NO and C/N_2O reaction. In situ XRD is used to identify the phases present under reaction conditions. This technique, combined with kinetic measurements, is a useful tool for interpreting catalyst behavior.

2. Experimental

Charcoal-activated GR MERCK (powder) was used to carry out isothermal kinetic studies and adsorption of NO and N_2O. This activated charcoal had a surface area of 1011 $m^2 g^{-1}$ and a pore total volume of 0.54 $cm^2 g^{-1}$. The charcoal was impregnated with diluted solutions of acetates of Mg, Mn, Ba, Pb, Cu, Ni, Fe, and Co. Metal salts were diluted in a small amount of distilled water, and the obtained solutions were added dropwise to the carbon, mixed thoroughly and the obtained product evaporated on hot plate. The metal loading was 4 wt.%.

In order to prevent diffusional limitations, thermogravimetric sample weight was 2–3 mg. Isothermal kinetic studies were carried out using a thermobalance system (CI Electronics MK II microbalance), with continuous recording of change in weight between 300°C and 900°C, with mixtures of Ar + 0.5% N_2O and Ar + 0.5% NO, with flow rates of 3.3 $cm^3 s^{-1}$.

For the adsorption studies, 10 mg of sample was weighed using the same apparatus, using 0.5% N_2O in Ar and 0.5% NO in Ar, with a flow rate of 3.3 $cm^3 s^{-1}$.

For comparison purposes, initial rates obtained at initial burn-off were used. The gassification rates at each temperature were derived from the relation

$$\mathrm{rate}\,(\mathrm{s}^{-1}) = \frac{(-\Delta w/\Delta t)}{w_o}$$

where w_o is the initial weight of the sample.

Before each experiment, Ar was introduced with a flow rate of 3.3 $cm^3 s^{-1}$, for 30 min, in order to

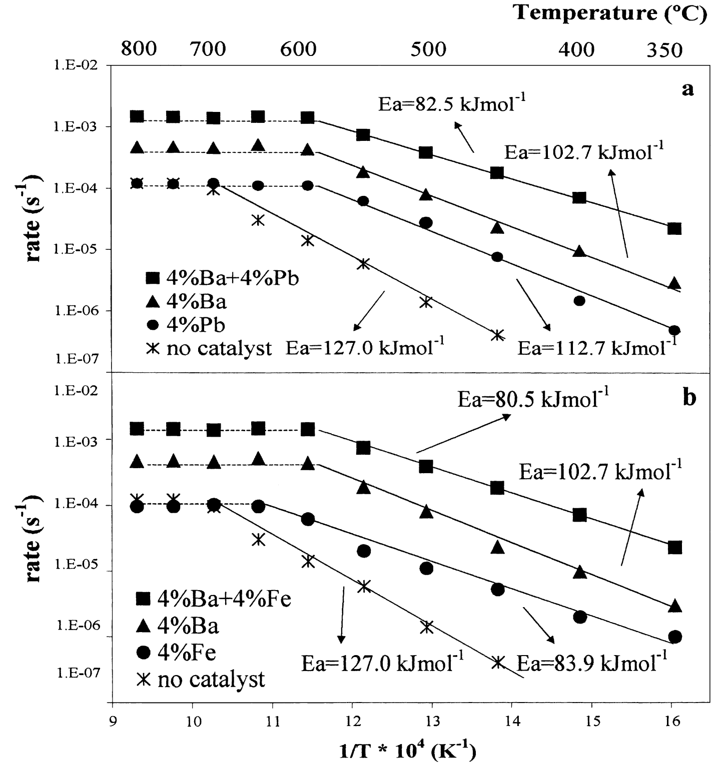

Fig. 3. Arrhenius plots for carbon gassification in N_2O for carbon parent sample and samples doped with Ba, Pb, and Ba + Pb mixture (a), and samples doped with Ba, Fe, and Ba + Fe mixture (b).

eliminate traces of air. The samples were heated in flowing Ar to 500°C to decompose precursor salts and eliminate volatiles adsorbed in carbon, until baseline sample weight was constant. The temperature was then adjusted to the desired value (20°C–900°C) and Ar was switched to NO or N_2O mixture.

The crystal phases detected by in situ XRD after pre-treatment in inert atmosphere at 500°C were MgO/MgO_2 for sample doped with Mg; Mn_3O_4/MnO_2 for sample doped with Mn; $BaCO_3/BaO/BaO_2/Ba$ for sample doped with Ba; Pb_3O_4/PbO for sample doped with Pb; CuO/Cu for sample doped with Cu; NiO/Ni for sample doped with Ni, Fe_2O_3/Fe_3O_4 for sample doped with Fe, and $Co_2O_4/CoO/Co$ for sample doped with Co.

In situ XRD studies were conducted in a Rigaku D/max III C diffractometer with a Cu (Ka) radiation source (50 kV, 30 mA), equipped with a high-temperature special chamber. All the experiments were carried out in exactly the same experimental conditions as in the thermogravimetric studies.

NO conversion was studied using a fixed-bed reactor. The reactor effluents were analyzed using a GC/MS (Fisons MD800) apparatus, equipped with a column of GS-Molesieve (30 m × 0.541 mm) type. These assays included heating of sample at 2°C min^{-1} (TPR) to 950°C in a mixture of 0.5% NO in He. The flow rate was 3.3 $cm^3\,s^{-1}$. All samples were pre-treated in He at 500°C for 30 min.

3. Results and discussion

NO and N_2O adsorption capacity increased considerably on adding metal catalysts when compared to the samples without catalyst, as shown in Fig. 1(a, b). An exception occurred for samples doped with Cu and Pb, which adsorbed less NO than parent sample, and also the sample doped with Fe, which adsorbed less N_2O than the sample with no catalyst. It has been shown that transition metals, like Co, Ni, Fe, Cu, and Ti, enhance NO adsorption [3–8,12,14].

The extent of enhancement depends on the kind of metal used. For NO adsorption, carbon samples doped with Co, Mn, Ba, and Ni showed maximum adsorption capacity. Adding another metal catalyst to the sample did not increase adsorption capacity.

Fig. 2(a, b) and Fig. 3(a, b) show the Arrhenius plots for NO and N_2O reactions. The kinetic results obtained suggest that activity for NO reduction is not only dependent on adsorption capacity, but also on the ability of the catalyst to be reduced by carbon and spread on the carbon surface, promoting catalyst dispersion. In the case of N_2O, activity is higher for the sample doped with Ba. Fig. 1(b) shows that sample doped with Ba exhibits higher adsorption capacity compared with Fe and Pb. The kinetic results obtained suggest that the activity depends on N_2O adsorption.

The values obtained for the apparent activation energies range from 149 $\mathrm{kJ\,mol^{-1}}$ to 70 $\mathrm{kJ\,mol^{-1}}$, and lie relatively well within those reported in the literature [3,13]. A substantial decrease in activation energy for the uncatalyzed (138 $\mathrm{kJ\,mol^{-1}}$) and Ba catalyzed reaction (74 $\mathrm{kJ\,mol^{-1}}$) in NO is observed.

Though N_2O is less adsorbed by carbon, it is more reactive than NO. N_2O seems to promote more less-stable oxygen surface complexes, which decompose yielding CO_2 and vacant sites. The presence of catalysts seems to favor the production of the surface-oxygen complexes, which, in turn, give rise to CO_2 and vacant sites, thus enhancing N_2O decomposition [3,9].

External diffusional limitations to mass transfer seem to take place in the reaction with N_2O above 600°C. A plateau is observed above 600°C at different reaction rates. These results suggest that addition of Ba seems to promote carbon particle diameter decrease, according to a shrinking-core model. Baker et al. reported in a previous study that barium oxide has the ability of melting and spreading on graphite oxidation and edge recession occurs [1]. As the interaction between carbon and catalyst is improved, the reaction takes place over a larger portion of the particle external surface. The observed reaction kinetics can also be explained by reaction transition from system gas–solid to system melt–solid. Reaction may be limited by the transfer of the N_2O species over the melt film (MxOy).

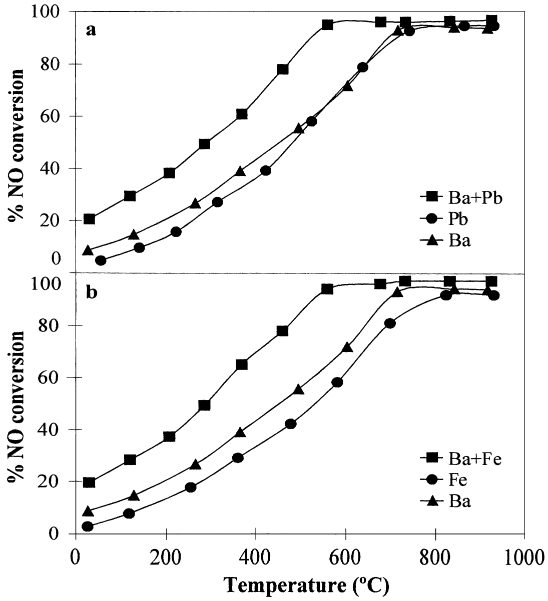

Fig. 4. NO conversion as a function of temperature (TPR) for samples doped with Ba, Pb, and Ba + Pb mixture (a), and samples doped with Ba, Fe, and Ba + Fe mixture (b).

Table 1 shows that synergetic effects for NO and N_2O reactions were observed for samples doped with the mixtures Ba + Cu, Ba + Mn, and Cu + Mn at higher and lower temperatures. Other mixtures with Ba showed synergetic effects only at higher temper-

Table 1
Initial gassification rates ($\times 10^5\,\mathrm{s^{-1}}$) in NO and N_2O at different temperatures for uncatalyzed and catalyzed reactions

	NO		N_2O	
	500°C	800°C	450°C	650°C
No catalyst	0.02	5.19	0.04	3.07
4% Ba	0.31	8.12	1.75	52.03
4% Pb	1.03	2.39	0.78	11.36
4% Ni	53.43	1.01	2.65	25.51
4% Fe	0.12	15.76	0.53	10.32
4% Mg	1.24	4.21	0.38	17.71
4% Cu	2.03	13.40	6.01	17.63
4% Mn	1.17	8.85	1.49	11.27
4% Co	2.51	33.34	5.77	47.88
4% V	0.67	5.17	0.62	16.36
4% Ba + 4% Mn	1.59	53.23	9.16	230.92
4% Ba + 4% Cu	5.68	51.11	18.99	124.57
4% Cu + 4% Mn	6.52	40.26	25.95	115.36

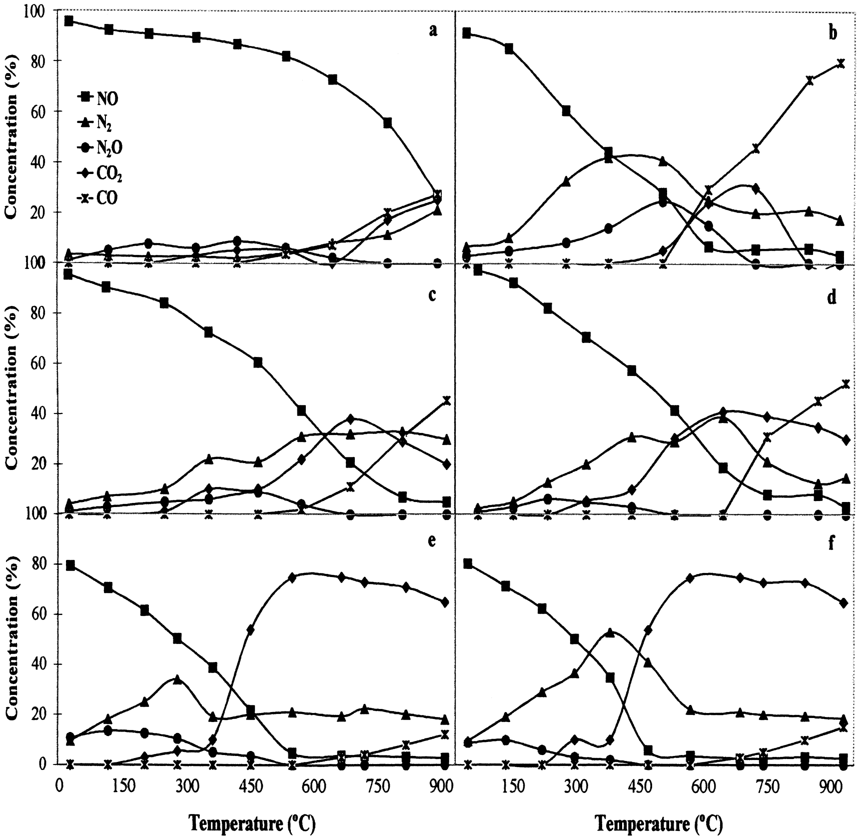

Fig. 5. Reaction products in TPR for carbon parent sample (a), and samples doped with Ba (b), Pb (c), Fe (d), Ba + Pb (e), and Ba + Fe (f) mixtures.

atures. Synergetic effects of binary mixtures were noted for catalytic gassification of carbon with steam. Melting of the catalysts and wetting of the carbon surface are important factors that affect the catalytic activity. The synergetic effects of binary mixtures can also result from other beneficial interactions between the mixture components and those between reactants and individual components [19]. The presence of Ba in the carbon surface seems to increase carbon reactivity at low temperatures. In situ XRD experiments carried out in nitrogen, the peak attributed to BaO/BaO_2 is clearly visible only after sample cooling. These observations suggest that BaO/BaO_2 is present as a melted phase. Melting of the catalysts improves wetting of the carbon surface promoting catalyst/carbon interaction [1,15,16,19].

Fig. 4(a, b) show the TPR profiles of samples doped with Ba + Pb and Ba + Fe, and Ba and Fe or Pb alone. Higher conversion of NO at lower temperatures is observed for the catalyst mixtures, in agreement with the results obtained in isothermal conditions.

The analysis of the reaction products using a GC/MS on line show the presence of N_2O, N_2, CO_2 and CO, together with some unreacted NO. For the single catalysts (Fig. 5(b–d)), only N_2 and N_2O were detected in the low-temperature range (20°C–300°C). Above 300°C, CO_2 is also observed. In the case of the binary mixtures, a substantial increase in CO_2 evolution was observed above 350°C. At higher temperatures, above 600°C or 700°C, N_2O emission ceases, and CO begins to appear. Similar results were obtained by other authors [3–7].In the presence of Pb and Fe (Fig. 5(c, d)), CO_2 evolution begins at lower temperatures, suggesting that the oxygen complexes are less stable and more abundant. Also, at low temperatures, an excess of N_2 is observed in contrast

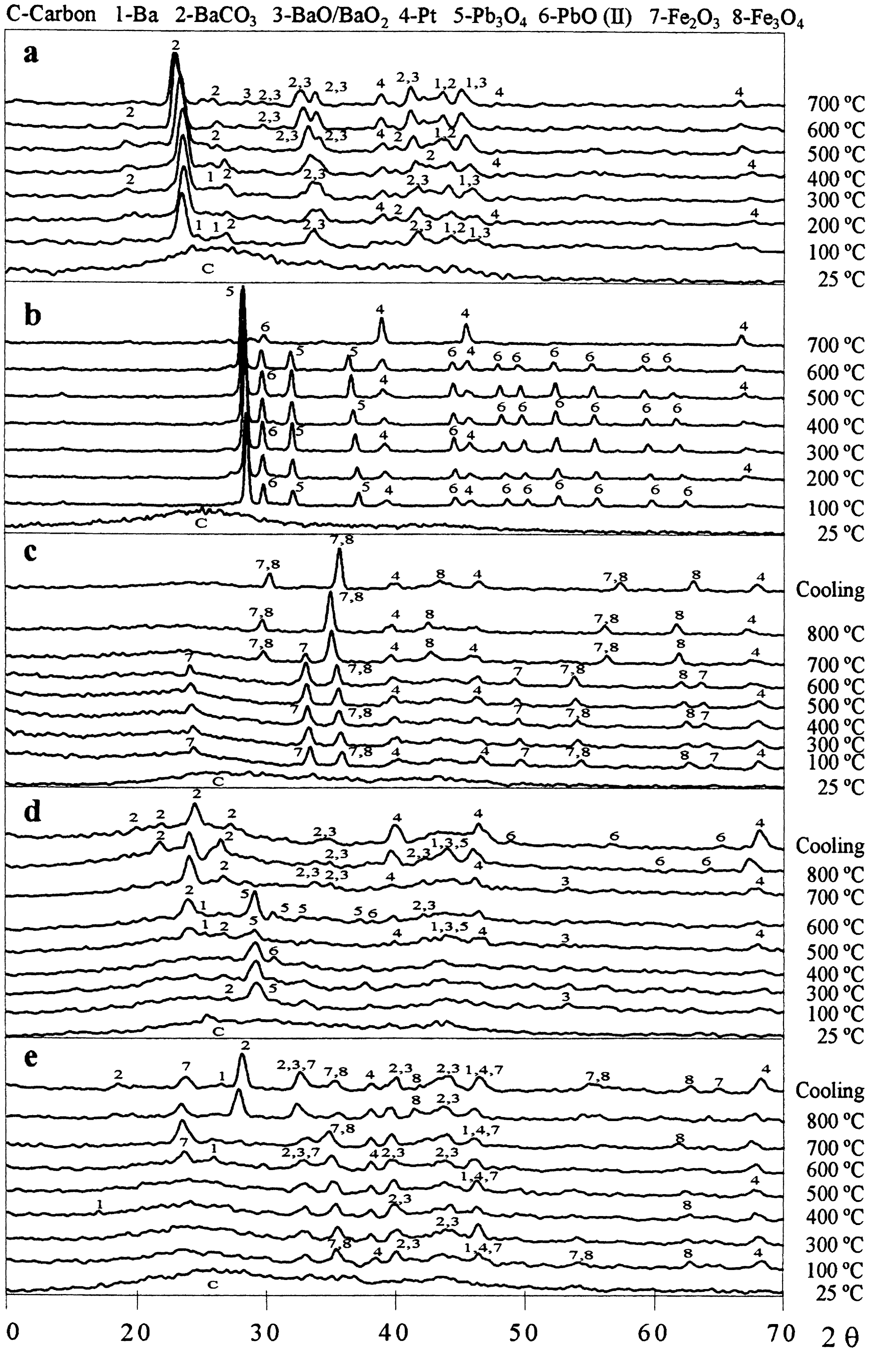

Fig. 6. In situ XRD data obtained from NO on heating samples doped with Ba (a), Pb (b), Fe (c), Ba + Pb (d), and Ba + Fe (e) mixtures at several temperatures.

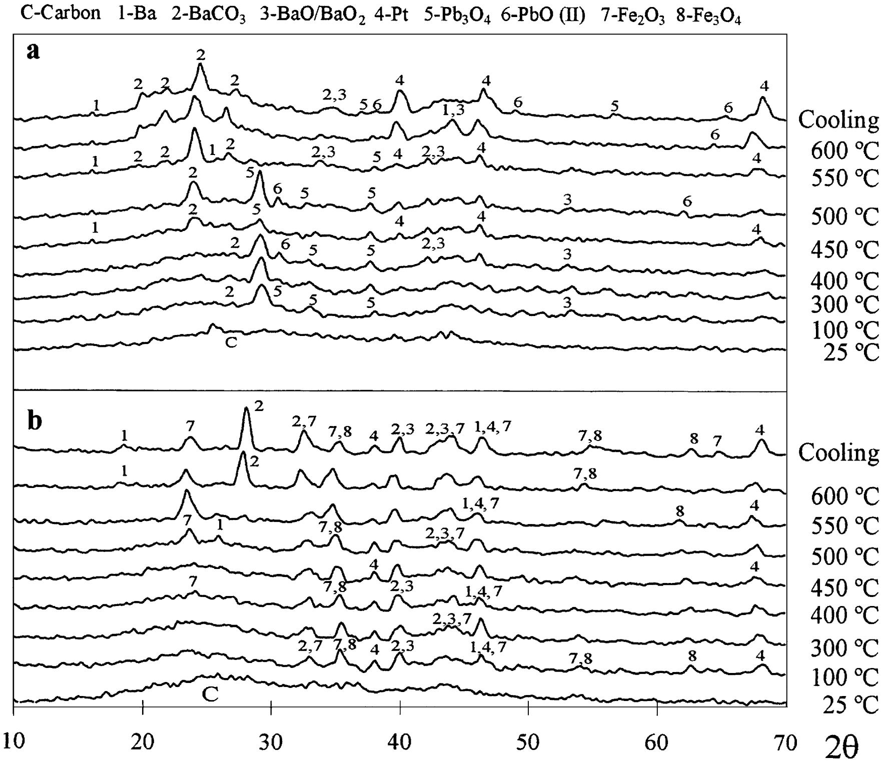

Fig. 7. In situ XRD data obtained from N_2O on heating samples doped with Ba + Pb (a) and Ba + Fe (b) mixtures at several temperatures.

with an excess of oxygen at higher temperatures. For mixtures (Fig. 5(e, f)), an increase in CO_2 evolution is observed. These results suggest that the synergetic effect observed for NO conversion is related to an increase in oxygen transfer to the carbon surface. The greater the rate of CO_2 evolution, the greater the NO conversion. As previously reported by Illán-Gomez et al. [4–8], the analysis of reaction products also reveals the three-stage mechanism for catalytic NO reduction already described in Section 1. In the case of N_2O decomposition, only N_2 and CO_2 were detected in agreement with the results referred to in the literature [3,9].

Active phases also play an important role in the catalytic conversion of NO. Fig. 6(a–e) and Fig. 7(a–b) show in situ XRD patterns obtained in NO and N_2O at several temperatures for carbon doped with the catalysts described above. Metal oxides are reduced to lower oxidation states. The peaks show shifts to 2θ with increasing temperature, which reflects expansion of the crystal lattices. Pt peaks appear in the spectra resulting from exposure to the sample holder to the X-ray beam as carbon burns away.

It has been reported recently that alkali, alkaline earth and transition metals enhance NO chemisorption. The catalytic system is more or less active depending on the ability of the oxide to be reduced by carbon and undergo redox reactions on the carbon surface [4–8]. The same mechanism has been proposed to explain carbon catalyzed reactions in other gaseous atmospheres [15–18].

In situ XRD shows clearly that catalysts are reduced to lower oxidation states, such as $BaCO_3$/BaO/BaO_2/Ba, Fe_2O_3/Fe_3O_4, and Pb_3O_4/PbO. The catalytic effect observed for the NO and N_2O conversion can be explained by the occurrence of redox processes, in which the oxides particles are reduced by reaction with the carbon at points of contact with the carbon substrate to form lower oxides according to a mechanism such as

$$\mathrm{Mx_{(s)}} + \mathrm{yNO_{(g)}} \rightarrow \mathrm{MxOy_{(s)}} + \frac{y}{2}\mathrm{N_{2(g)}}$$

$$\mathrm{MxOy_{(s)}}\frac{y}{2}\mathrm{C_{(s)}} \rightarrow \mathrm{Mx_{(s)}} + \frac{y}{2}\mathrm{CO_{2(g)}}$$

TPR results show that in the case of Ba and the mixtures, CO_2 evolution is delayed with respect to N_2. This behavior was also observed to a less extent in the case of Fe. This delay may be due to the fact that the catalyst retains the oxygen produced by the dissociative NO chemisorption. The evolution of CO_2 allows the catalyst to continue transferring oxygen from NO or N_2O to carbon, generating new active sites on the carbon surface.

The reduction temperature of the metal oxide seems to be a key factor controlling the activity of the metal as catalyst. Illán-Gomez et al. reported that a relationship exists between the ease of the oxidation–reduction (to metallic or lower oxidation state) and the lattice energy of oxide or the free energy of oxide formation [7]. When TPR experiments were performed after NO chemisorption, N_2 and/or N_2O were not observed at low temperatures [8]. The catalyst became inactive due to its conversion to the oxidized state and negligible NO reduction took place. It was only when CO_2 evolution began that NO reduction occurred on an oxygen-saturated surface [8]. In our work, it was shown by in situ XRD that after pre-treatment at 500°C in inert atmosphere, the catalysts were already reduced by carbon to lower oxidation states.

Another important factor is catalyst dispersion. As the catalyst dispersion increases, the process of oxidation and reduction of the catalyst is enhanced because the redox mechanism occurs at the catalyst/carbon interface. Thus, in the case of the samples doped with Ba, the catalyst/carbon interaction is promoted because the catalyst seems to be present as a melted phase.

In situ XRD shows the probable species involved in the reaction conditions. It seems that a reduced catalyst surface is then required for NO and N_2O reduction. The active catalysts seem to act as an oxygen acceptor from NO or N_2O, transferring it to the carbon surface, thus recovering the reduced state. Similar behavior has been reported by several authors. [4–8,10,11].

4. Conclusions

This study has indicated that kinetic measurements, combined with in situ XRD, are a useful tool for interpreting catalyst behavior. In the C–NO and C–N_2O reaction, a reduced catalyst surface is required for NO and N_2O reduction.

The ability of the catalyst to chemisorb NO going through redox transference of oxygen to the carbon reactive sites seems to explain the catalytic activity.

The synergetic effect observed with addition of Ba seems to be related with an enhancement of oxygen–carbon complexes and CO_2 evolution.

Acknowledgements

Sónia Carabineiro acknowledges financial support from Fundação para a Ciência e Tecnologia, Grant BD1275/95.

References

[1] R.T.K. Baker, C.R.F. Lund, J.J. Chlundzinski Jr., J. Cat. 87 (1984) 255.
[2] T. Okuhara, K. Ichi Tamaka, J. Chem. Soc., Faraday Trans. 82(1) (1986) 3657.
[3] J. Rodriguez-Mirasol, A. Ooms, J. Pels, F. Kapteijn, J. Moulijn, Combust. Flame 99 (1994) 499.
[4] M.J. Illán-Gomez, C. Salinas-Martinez de Lecea, A. Linares-Solano, in: Proc. Carbon 94, Granada, Spain, 3–8 July 1994, p. 460.
[5] M.J. Illán-Gomez, A. Linares-Solano, L. Radovic, C. Salinas-Martinez de Lecea, Ener. Fuels 9 (1995) 97.
[6] M.J. Illán-Gomez, A. Linares-Solano, L. Radovic, C. Salinas-Martinez de Leccea, Ener. Fuels 9 (1995) 540.
[7] M.J. Illán-Gomez, A. Linares-Solano, C. Salinas-Martinez de Lecea, Ener. Fuels 9 (1995) 976.
[8] M.J. Illán-Gomez, A. Linares-Solano, L. Radovic, C. Salinas-Martinez de Lecea, Ener. Fuels 10 (1996) 158.
[9] J. Rodriguez-Mirasol, J. Pels, F. Kapteijn, J. Moulijn, in: Proc. 22nd Bi. Conf. Carbon, San Diego, CA, 16–21 July 1995, p. 620.
[10] D. Mehardjeive, M. Khristova, E. Bekyarova, Carbon 34 (1996) 757.
[11] C. Marquez-Alvarez, I. Rodriguez-Ramos, Guerrero-Ruiz, Carbon 34 (1996) 339.
[12] S. Carabineiro, I.F. Silva, F.B. Fernandes, in: Proc. 9th Int. Conf. Coal Science, vol. 2, Essen, Germany, 7–12 September 1997, p. 1103.
[13] I. Aarna, E. Suuberg, Fuel 76 (1997) 475.
[14] S. Carabineiro, I.F. Silva, F.B. Fernandes, A.M. Ramos, J.S. Vital, in: Proc. Eurocabon 98, vol. 1, Strasbourg, France, 5–9 July 1998, p. 411.
[15] D.W. McKee, Chemistry and Physics of Carbon, vol. 16, 1, Marcel Dekker, New York, 1981, p. 1.
[16] D.W. McKee, Carbon 8 (1970) 623.
[17] I.F. Silva, L.S. Lobo, J. Cat. 126 (1990) 489.
[18] I.F. Silva, D. Mckee, L.S. Lobo, J. Cat. 170 (1997) 54.
[19] I.F. Silva, C. Palma, M. Klimkiewicz, S. Eser, Carbon 36 (1998) 861.